

# Kinematic Modeling and Workspace Analysis of a Spatial Cable Suspended Robot as Incompletely Restrained Positioning Mechanism

. Jahanbakhsh Hamed, and Hassan Zohoor

**Abstract**—This article proposes modeling, simulation and kinematic and workspace analysis of a spatial cable suspended robot as incompletely Restrained Positioning Mechanism (IRPM). These types of robots have six cables equal to the number of degrees of freedom. After modeling, the kinds of workspace are defined then an statically reachable combined workspace for different geometric structures of fixed and moving platform is obtained. This workspace is defined as the situations of reference point of the moving platform (center of mass) which under external forces such as weight and with ignorance of inertial effects, the moving platform should be in static equilibrium under conditions that length of all cables must not be exceeded from the maximum value and all of cables must be at tension (they must have non-negative tension forces). Then the effect of various parameters such as the size of moving platform, the size of fixed platform, geometric configuration of robots, magnitude of applied forces and moments to moving platform on workspace of these robots with different geometric configuration are investigated. Obtained results should be effective in employing these robots under different conditions of applied wrench for increasing the workspace volume.

**Keywords**—Kinematic modeling, applied wrench, workspace, cable based robot.

## I. INTRODUCTION

CABLE robots are a group of parallel robots, which cables and winches are used instead of links and actuators, respectively. The moving platform connects to the fixed platform by some cables. For the first time, study about these robots was presented about 18 years ago [1]. because of light weight of cables, they are suitable for high speeds applications. Also they have large workspace volume. The study has been done on cable robots in order to heavy loads handling such as cranes [2], purposes of the very high velocity and acceleration [3], kinematics and statics [4, 5].

Jahanbakhsh Hamed is Phd student with Islamic Azad University, Science and Research Branch, Tehran, Iran and Lecturer with Islamic Azad University, Central Tehran Branch, Tehran, Iran. e-mail: [jbhamed@iauctb.ac.ir](mailto:jbhamed@iauctb.ac.ir)

Hassan Zohoor is Distinguished Professor and Member, with Center of Excellence in Design, Robotics and Automation, School of Mechanical Engineering, Sharif University of Technology, Tehran, Iran and Secretary, The Academy of Sciences of IR, P.O.Box 19735-167, 19 Shahmoradi Lane, Darband Ave., Tajrish, 19717, Tehran, Iran, e-mail: [zohoor@sharif.edu](mailto:zohoor@sharif.edu)

Notice to importance of workspace in these robots, different studies has been done in this context [6-9].

Study on applied wrench (forces and moments) feasible workspace has got a particular significant and quantitative studies have been done in this context. From the quantity of cables and number of degrees of freedom viewpoint, cable robots are divided to three categories [6] that each has its own special advantages. Meanwhile, incompletely restrained positioning mechanism is used mostly for lifting and transportation of heavy loads and the maximum number of cables are equal to the number of degrees of freedom. Notice to this fact that concentration of this study is on heavy loads handling so geometric structures of IRPM cable robots with six degrees of freedom and six cables is used as each motor is used to control one cable and totally six motors used for six cables. In this research we tried to fill a need for workspace volume and endurance sufficiency of applied wrenches to moving platform in these robots.

This paper has been divided into different sections as follows: Section 2 refers to the geometric and kinematic modeling of the robot including selection of proper geometrical pattern for load handling and description of used equations and variables. In section 3 the effects of various parameters on workspace is simulated. After defining the different kinds of workspace, the effects of various parameters such as sizes of the moving platform (MP) and the fixed platform (BP) on the workspace are investigated. In section 4 the effects of applied wrench to end-effector (moving platform) on workspace is analyzed.

## II. GEOMETRIC AND KINEMATIC MODELING

The geometric model used in this paper is IRPM model with six degrees of freedom and six cables as each motor is used to control one cable and totally six motors to control six cables and is shown in Fig. 1.  $O_F$  is the center of the fixed inertia coordinates XYZ which coincides with the surface center of base platform (BP),  $O_M$  is the center of principal body coordinates xyz which coincides with the center of mass of moving platform (MP),  $r_{base}$  is the radius of points of connection of the cables to the base platform from the reference point  $O_F$  (surface center of base platform) and  $r_{end}$  is the radius of points of connection of the cables to moving

platform from the reference point  $O_M$  (center of mass of the moving platform).  $\gamma$  is the angle between the BP connection points, i.e.  $(C_2, C_1)$ ,  $(C_3, C_4)$ ,  $(C_5, C_6)$ , and MP connection points, i.e.  $(D_1, D_6)$ ,  $(D_2, D_3)$ ,  $(D_4, D_5)$ . Figs. 2 and 3 represent  $\gamma$  angle for fixed and moving platform respectively. It is obvious that both of MP and BP configurations for  $\gamma=45^\circ$  and  $\gamma=0^\circ$  are a symmetrical hexagon and similar equilateral triangles with Stewart platform respectively.

From the polygon of vectors shown in Fig. 4 we can derive the following relation:

$$\vec{l}_i = \vec{r} + [R]^M \vec{d}_i - \vec{c}_i \quad i = 1, \dots, 6 \quad (1)$$

$c_i$ : Position vector of point  $C_i$  (with components  $C_i(X_{C_i}, Y_{C_i}, Z_{C_i})$ )

$d_i$ : Position vector of point  $D_i$  (with components  $D_i(X_{D_i}, Y_{D_i}, Z_{D_i})$ )

$r$ : Position vector of point  $O_M$  center of moving platform (X, Y and Z components in fixed frame)

$l_i$ : Distance between  $C_i$  and  $D_i$  ( $l_{ith}$  cable length)

$R$  is the moving platform rotation matrix with respect to base platform with rotation angles  $\psi, \theta, \phi$  respectively about inertia coordinate axes of moving platform X, Y and Z:

$$R = \begin{bmatrix} \cos\phi \cos\theta & -\sin\phi \cos\psi + \cos\phi \sin\theta \sin\psi & \sin\phi \sin\psi + \cos\phi \sin\theta \cos\psi \\ \sin\phi \cos\theta & \cos\phi \cos\psi + \sin\phi \sin\theta \sin\psi & -\cos\phi \sin\psi + \sin\phi \sin\theta \cos\psi \\ -\sin\theta & \cos\theta \sin\psi & \cos\theta \cos\psi \end{bmatrix} \quad (2)$$

The length of the cables (magnitude of each vector  $\vec{l}_i$ ) is:

$$l_i = \|\vec{l}_i\| = (\vec{l}_i^T \vec{l}_i)^{1/2} \quad (3)$$

However, posture of the moving platform (end-effector) is:

$$u = [x \ y \ z \ \psi \ \theta \ \phi]^T \quad (4)$$

According to definition, inverse jacobian is a matrix which transforms MP velocity to cable velocity and we have:

$$J_{ij} = \frac{\partial q_i}{\partial u_j} \quad (5)$$

Thus Jacobian matrix defines the imaginary displacement of moving platform  $\delta u$  and imaginary displacement of cables  $\delta q$ , and they are relating to each other with equation below:

$$\delta q = J \delta u \quad (6)$$

Cable based robots move via servomotors that control the tension in cables. Because all the cables connect to moving platform, forces in moving platform are directly proportional to amount and direction of tension cables by Jacobian matrix.

In order to calculate the tension in cables, we use equation (7):

$$J^T s = f_{\text{ext}} \quad (7)$$

Where  $s$  is vector of the cable stress,  $f_{\text{ext}}$  is the vector of external wrench applied to the moving platform and  $J^T$  is the Jacobian matrix (structure matrix) as follows:

$$J^T = \begin{bmatrix} \left( \frac{\vec{l}_1}{|\vec{l}_1|} \right)^T \left( {}^B \vec{d}_1 \times \frac{\vec{l}_1}{|\vec{l}_1|} \right)^T \\ \vdots \\ \left( \frac{\vec{l}_m}{|\vec{l}_m|} \right)^T \left( {}^B \vec{d}_m \times \frac{\vec{l}_m}{|\vec{l}_m|} \right)^T \end{bmatrix} \quad (8)$$

Where:

$${}^B \vec{d}_i = \vec{r} + [R]^M \vec{d}_i \quad (9)$$

### III. WORKSPACE ANALYSIS

In case of importance of workspace in cable robots, first we define the workspace. Workspace divided to different categories [6-10]. One of the most important workspaces is the statically reachable combined workspace. This workspace is consist of poses of end-effector reference point (mass center) which under applied external forces such as weight and ignoring inertial effects, end-effector should be in static equilibrium, the length of all the cables should be smaller than maximum amount and all the cables should be in tension (nonnegative stress) while rotation of the end-effector in some of the constant rotation angles of  $\psi, \theta$  and  $\phi$  is possible.

Where the rotation angles  $\psi, \theta$  and  $\phi$  are rotation angles around fixed axes of moving platform X, Y and Z respectively. In some cases we call this workspace, wrench feasible workspace. This workspace is consisting of all the poses of moving platform that we can apply a specific range of wrenches (forces/moments).

Anyway we can divide this space to two categories, the first is constant orientation workspace and the second is total orientation workspace.

Constant orientation workspace is the one that  $O_M$  point (mass center of MP) from MP can be available while orientation of end-effector should be possible in some constant orientation angles  $\psi, \theta$  and  $\phi$ .

Total orientation workspace (sometimes we can call workspace dexterous) is consist of space in which  $O_M$  point from MP can be available while orientation of end-effector should be possible in all constant orientation angles  $\psi, \theta$  and  $\phi$ . Of course it is obvious that this workspace is a subset of constant orientation workspace.

In this section notice to the importance of the statically reachable combined workspace in cable robots, we obtain this space for different geometrical structure of fixed and moving

platforms (different  $\gamma$  angles) and also we study the effect of different parameters on it.

Because all the cables can sustain tension and cannot sustain pressure in all of moving platform positions, all the cables should have no negative stresses. In addition we suppose all the cables are not elastic and they make a straight line between base joint point and joint point of moving platform.

Different programs were written by use of MATLAB software. This programs checks all the points of search space for calculating the workspace, with respect to range of search that is cube consist of numerous number of points and attain due to search step and under following conditions:

$$\left\{ \begin{array}{l} s = J^{-T} f_{ext} \\ s \in [s_{min}, s_{max}] \\ s_i \geq 0 \therefore i = 1, \dots, 6 \end{array} \right. \quad \text{and} \quad l_i \leq l_{max} \quad (10)$$

Obtains the statically reachable points and such set comprises statically reachable combined workspace. Desired assumptions as follows:

- 1)  $r_{base}=6m$  radius of connected points of cables to base from reference point  $O_F$ .
- 2)  $r_{end}$  radius of joint points of cables to moving platform from reference point  $O_M$  (mass center of moving platform).
- 3)  $l_{max}=15m$ , maximum length of cables.
- 4)  $0 \leq Z \leq 10, -6 \leq Y \leq 6, -6 \leq X \leq 6$  (m) desired search range
- 5)  $\Delta X = \Delta Y = \Delta Z = 0.4m$ , size of search step in direction of each three axis.
- 6)  $\gamma = 0^\circ, 15^\circ, 30^\circ, 45^\circ$
- 7)  $f_{ext} = [0 \ 0 \ 100 \ 0 \ 0 \ 0]^T$  KN vector of applied wrench to moving platform.
- 8)  $s_{max} = 55$  KN maximum sustainable tension force of cables.

Now we obtain statically reachable combined workspace for different geometric structures of fixed and moving platforms (different  $\gamma$  angles).

#### A. The Effect of Various Ratios of MP/BP (with Constant BP Size) on the Workspace Volume

The size of MP with respect to BP is varied from lower sizes to equivalent BP size. We consider size of BP as constant,  $r_{base}=6m$  and the rotation of moving platform constant and equal to zero ( $\psi=0, \theta=0, \phi=0$ ). The variations are considered for four different geometries consisting of  $\gamma=0^\circ, 15^\circ, 30^\circ, 45^\circ$ . The results of simulation for two ratios ( $r_{end}/r_{base}$ ) = 0.2, 1 and for all geometrical configurations  $\gamma=0^\circ, 15^\circ, 30^\circ, 45^\circ$  are drawn in Figs. 5 to 12. The number of points obtained for these configurations in all ratios of ( $r_{end}/r_{base}$ ) are 3675, 2500, 1375, 375 points for  $\gamma=0^\circ, \gamma=15^\circ, \gamma=30^\circ$  and  $\gamma=45^\circ$  respectively.

Fig. 13 shows the variations of ( $r_{end}/r_{base}$ ) on the basis of workspace volume for all ratios of ( $r_{end}/r_{base}$ ) = 0.2, 0.4, 0.6, 0.8, 1. As shown in the graph we can conclude when size of BP is constant and ratio of MP to BP changes, the workspace volume remains constant. In other words the statically reachable combined workspace volume with zero rotation of MP is independent of the size of MP. But reduction in angle  $\gamma$  results in the increase of workspace.

#### B. The Effect of Various Sizes of BP (having constant MP size) on the Workspace Volume

In this section the size of MP with respect to BP is constant but size of BP varies (reverse of 3.1 case). The size of BP varies from smaller to larger quantities. The variations are applied to four different geometries consisting of  $\gamma=0^\circ, 15^\circ, 30^\circ, 45^\circ$ . The results in Fig. 14 are obtained for constant rotation ( $\psi=0, \theta=0, \phi=0$ ). As it is apparent from figure when size of BP is changed, workspace volume increases.

#### C. The Effect of Various Ratios of BP/MP (with Constant MP Size) on the Workspace Volume

In this section the size of BP with respect to MP is changed from smaller to larger sizes (we consider size of MP as constant and  $r_{end}=0.6m$ ). For four different geometries consisting of  $\gamma=0^\circ, 15^\circ, 30^\circ, 45^\circ$ , search is conducted. Fig. 15 shows the graph of variations of ( $r_{base}/r_{end}$ ) based on workspace volume for ratios of ( $r_{base}/r_{end}$ ) = 0.2, 0.4, 0.6, 1 and under the condition of constant rotation ( $\psi=0, \theta=0, \phi=0$ ). As it is apparent from the graph when size of MP is constant and ratio of BP/MP changes, the workspace varies according to the graph and for maximum workspace the limit of ( $r_{base}/r_{end}$ )=1 does not exist. As a result the volume of statically reachable combined workspace with zero rotation of MP, increases as the ratio of ( $r_{base}/r_{end}$ ) is increased. Simultaneously, decrease in angle  $\gamma$  also leads to increase of workspace.

## IV. SOME COMMON MISTAKES

The applied external wrench to the end-effector is in the form of a column vector with six components (three forces in the direction of three axes and three moments about three axes with coordinate center coinciding with the center of mass of moving platform). In the previous sections, the only applied force to the end-effector was considered the applied weight force to the center of mass in the direction of z axis. But in this section, the effects of variations of applied forces and moments to the end-effector on the workspace are discussed. As it was also indicated in section 3, these types of workspace are known as wrench feasible workspace. The vector of applied external wrench is assumed as follows:

$$f_{ext} = [f_x \quad f_y \quad f_z \quad M_{yz} \quad M_{xz} \quad M_{xy}]^T \quad (11)$$

while  $f_x$ ,  $f_y$  and  $f_z$  are applied forces to MP in directions x, y and z axes respectively and  $M_{yz}$ ,  $M_{xz}$  and  $M_{xy}$  are applied moments to MP about three axes x, y and z respectively.

#### A. The Effect of Variations in the Forces $f_x$ and $f_y$ , Sizes of MP and BP and Angle $\gamma$ on Workspace Volume

Initially, we consider force  $f_z$  is constant and equal to 100 KN and all moments to be zero, by holding  $r_{base}=6m$  constant and for three cases of  $(r_{end}/r_{base})=1$ ,  $(r_{end}/r_{base})=0.8$  and  $(r_{end}/r_{base})=0.6$ , the magnitude of forces  $f_x$  and  $f_y$  are changed and their effects on the workspace are investigated. Figs. 16 to 18 show the results of workspace calculation for all configurations of  $\gamma=0^\circ, 15^\circ, 30^\circ, 45^\circ$ . The relevant curve to  $\gamma=0^\circ$  be the topmost curve and respectively downwards related curves to the angles  $15^\circ, 30^\circ, 45^\circ$  are shown. It is clear that by holding  $r_{base}$  constant, reduction of forces  $f_x$  and  $f_y$  results in the increase of workspace and on the other hand the changes in the parameter  $(r_{end}/r_{base})$  do not have any effect on the wrench feasible workspace volume. This result is also valid for any other ratios of  $(r_{end}/r_{base})$ . Hence changes in the size of MP under these conditions have no effects on the wrench workspace.

In order to show the effects of BP size on the wrench feasible workspace, once again like previous case the force  $f_z$  is considered as constant and equal to 100 KN but with this difference that in this case instead of holding  $r_{base}$  constant, the size of  $r_{end}$  is considered constant and  $r_{end}=6m$ . As the results show, for the configuration  $\gamma=45^\circ$  with ratios of  $(r_{base}/r_{end})=0.2, 0.4, 0.6$  no workspace is available, so for two states of  $(r_{base}/r_{end})=0.8$  and  $(r_{base}/r_{end})=0.6$ , the magnitude of forces  $f_x$  and  $f_y$  are changed and their effects on workspace are checked. Figs. 19 and 20 show the results of workspace calculation for all configurations of  $\gamma=0^\circ, 15^\circ, 30^\circ, 45^\circ$ . The relevant curve to  $\gamma=0^\circ$  be the topmost curve and respectively downwards related curves to the angles  $15^\circ, 30^\circ, 45^\circ$  are shown. It is observed that by holding  $r_{end}$  constant, reduction of forces  $f_x$  and  $f_y$  leads to the increase in workspace and on the other hand changes in parameter  $(r_{base}/r_{end})$  contrary to  $(r_{end}/r_{base})$  have significant influence on the wrench feasible workspace. This result is also valid for any other ratios of  $(r_{base}/r_{end})$ . Hence reduction in forces  $f_x$  and  $f_y$  increases the size of BP (increase of ratio  $(r_{base}/r_{end})$ ) and reduction of angle  $\gamma$  increases the workspace under these conditions.

#### B. The Effect of Variations in the Forces $f_y$ and $f_z$ , Sizes of MP and BP and Angle $\gamma$ on Workspace Volume

Initially, we consider that force  $f_x$  is constant and equal to 100 KN and all moments to be zero, by holding  $r_{base}=6m$  constant and for two states of  $(r_{end}/r_{base})=1$  and  $(r_{end}/r_{base})=0.6$ , the magnitude of forces  $f_y$  and  $f_z$  are changed and their effects on the workspace are examined. Figs. 21 and 22 show the

results of workspace calculation for all configurations of  $\gamma=0^\circ, 15^\circ, 30^\circ, 45^\circ$ . The relevant curve to  $\gamma=0^\circ$  be the topmost curve and respectively downwards related curves to the angles  $15^\circ, 30^\circ, 45^\circ$  are indicated. It is observed that by holding  $r_{base}$  constant, reducing the force  $f_y$  and increasing the force  $f_z$  results in the increase of workspace and on the other hand the changes in the parameter  $(r_{end}/r_{base})$  does not have any effects on the volume of wrench feasible workspace. This result is also valid for any other ratios of  $(r_{end}/r_{base})$ . Hence changes in the size of MP under these conditions have no effects on the wrench workspace.

In order to show the effects of BP size on the wrench feasible workspace, again similar to previous case the force  $f_x$  is considered as constant and equal to 100 KN but with this difference that in this case instead of considering  $r_{base}$  as constant, the size of  $r_{end}$  is held constant and  $r_{end}=6m$ . For the case of  $(r_{base}/r_{end})=0.6$ , we change the magnitude of forces  $f_y$  and  $f_z$  and their effects on the workspace are studied. Fig. 23 shows the results of workspace calculation for all configurations of  $\gamma=0^\circ, 15^\circ, 30^\circ, 45^\circ$ . The relevant curve to  $\gamma=0^\circ$  is the topmost curve and respectively downwards related curves to the angles  $15^\circ, 30^\circ, 45^\circ$  are shown. It is observed that like the previous case by holding  $r_{end}$  constant, reduction of force  $f_y$  and increase of force  $f_z$  results in the increase in workspace, but on the other hand variations in parameter  $(r_{base}/r_{end})$  contrary to  $(r_{end}/r_{base})$  have a considerable effect on the wrench feasible workspace. This result is also valid for any other ratios of  $(r_{base}/r_{end})$ . Hence reducing the force  $f_y$  and increasing the force  $f_z$ , increases the size of BP (increase of ratio  $(r_{base}/r_{end})$ ) and reduction of angle  $\gamma$  results in the increase of workspace under these conditions.

#### C. The Effect of Variations in the Forces $f_x$ and $f_z$ , Sizes of MP and BP and Angle $\gamma$ on Workspace Volume

In this case also if the force  $f_y$  is held constant and equal to 100 KN and all moments equal to zero, by holding  $r_{base}=6m$  as constant and for various ratios of  $(r_{end}/r_{base})$ , the magnitude of forces  $f_x$  and  $f_z$  are varied and their effects on the workspace are studied. Exactly same results as case 4.2 are obtained (by replacing  $f_x$  with  $f_z$ ). The all of Figures in this case are the same as 4.2 case. In order to avoid excessive number of graphs and repetition, we have disregarded presenting curves and have sufficed in stating the results. As result by holding  $r_{base}$  constant, reducing the force  $f_x$  and increasing the force  $f_z$  leads to the increase of workspace and on the other hand the changes in the parameter  $(r_{end}/r_{base})$  does not have any influences on the volume of wrench feasible workspace. This result is also valid for any other ratios of  $(r_{end}/r_{base})$ . Hence changes in the size of MP under these conditions have no effects on the wrench workspace.

Also by holding  $r_{end}$  constant, reduction of force  $f_x$  and increase in force  $f_z$ , increases the workspace but on the other hand variations in parameter  $(r_{base}/r_{end})$  contrary to  $(r_{end}/r_{base})$  have a considerable effect on the wrench feasible workspace. This result is also valid for any other ratios of  $(r_{base}/r_{end})$ .

Hence reducing the force  $f_x$  and increasing the force  $f_z$ , increases the size of BP (increase of ratio  $(r_{base}/r_{end})$ ) and reduction of angle  $\gamma$  results in the increase of workspace under these conditions.

#### D. The Effect of Variations in the Forces $M_x$ and $M_y$ , Sizes of MP and BP and Angle $\gamma$ on Workspace Volume

Initially, we consider that moment  $M_z$  is constant and equal to 100 KN.m and all forces are constant and equal to 100 KN, by holding  $r_{base}=6m$  constant and for two states of  $(r_{end}/r_{base})=1$  and  $(r_{end}/r_{base})=0.6$ , the magnitude of moments  $M_x$  and  $M_y$  are varied and their effects on the workspace are studied. Figs. 24 and 25 show the results of workspace calculation for all configurations of  $\gamma=0^\circ, 15^\circ, 30^\circ, 45^\circ$ . The relevant curve to  $\gamma=0^\circ$  be the topmost curve and respectively downwards related curves to the angles  $15^\circ, 30^\circ, 45^\circ$  are indicated. These figures also show the drastic reduction in the workspace under the condition of bearing moments  $M_x$  and  $M_y$ . It can be observed by holding  $r_{base}$  constant, reduction of moments  $M_x$  and  $M_y$  results in the increase of workspace and on the other hand the changes in the parameter  $(r_{end}/r_{base})$  contrary to sections 4.1 to 4.3 have positive effects on the volume of wrench feasible workspace, any increase in it leads to increase of workspace.

In order to indicate the effects of size of BP on the wrench feasible workspace, again similar to previous case the moment  $M_z$  is considered as constant and equal to 100 KN.m but with this difference that in this case instead of holding  $r_{base}$  constant, the size of  $r_{end}$  is held constant and we select  $r_{end}=6m$ . For the state of  $(r_{base}/r_{end})=0.6$ , the magnitude of moments  $M_x$  and  $M_y$  are changed and their effects on the workspace are studied. Fig. 26 indicates the results of workspace calculation for all configurations of  $\gamma=0^\circ, 15^\circ, 30^\circ, 45^\circ$ . The pertinent curve to  $\gamma=0^\circ$  be the topmost curve and respectively downwards related curves to the angles  $15^\circ, 30^\circ, 45^\circ$  are shown. It is seen that by holding  $r_{end}$  constant, reduction of moments  $M_x$  and  $M_y$  results in the increase of workspace and on the other hand changes in parameter  $(r_{base}/r_{end})$  have influence on the volume of wrench feasible workspace. This result is also valid for any other ratios of  $(r_{base}/r_{end})$ . Hence reduction in moments  $M_x$  and  $M_y$  increases the size of BP (increase of ratio  $(r_{base}/r_{end})$ ) and the size of MP (increase of ratio  $(r_{end}/r_{base})$ ), and simultaneously reduction of angle  $\gamma$  increases the workspace considerably under these conditions.

#### E. The Effect of variations in the forces $M_y$ and $M_z$ , sizes of MP and BP and angle $\gamma$ on workspace volume

If we consider moment  $M_x$  is constant and equal to 100 KN.m and all forces as constant and equal to 100 KN, by holding  $r_{base}=6m$  constant and for two states of  $(r_{end}/r_{base})=1$  and  $(r_{end}/r_{base})=0.6$ , we vary the magnitude of moments  $M_y$  and  $M_z$  and then obtain the curves of Figs. 27 and 28 which have the similar results to the case (3-4) above by replacing  $M_z$  by  $M_x$ . These figures also indicate that workspace within the

limits of slight variations of  $M_y$ , exists in the vast range of changes of  $M_z$ .

In order to show the effects of size of BP on the wrench feasible workspace, once again like previous case the moment  $M_x$  is considered as constant and equal to 100 KN.m but with this difference that in this case instead of holding  $r_{base}$  constant, the size of  $r_{end}$  is held constant and is considered  $r_{end}=0.6$ . For the state of  $(r_{base}/r_{end})=0.6$ , the magnitude of moments  $M_y$  and  $M_z$  are changed and their effects on the workspace are studied. Fig. 29 indicates the results of workspace calculation for all configurations of  $\gamma=0^\circ, 15^\circ, 30^\circ, 45^\circ$  which gives similar results to the case 4.4 and are obtained by replacing  $M_z$  by  $M_x$ .

#### F. The Effect of Variations in the Forces $M_x$ and $M_z$ , Sizes of MP and BP and Angle $\gamma$ on Workspace Volume

If we consider moment  $M_y$  is constant and equal to 100 KN.m and all forces are constant and equal to 100 KN, similar results to the case 4.5 are obtained by replacing  $M_y$  with  $M_x$ . Hence we have disregarded presenting the curves.

## V. CONCLUSION

With respect to the curves obtained in sections 3 and 4 we can arrive at the following results:

1) The statically reachable combined workspace volume with zero rotation of MP is independent of the size of the MP and any changes in the ratio of MP/BP have no effects on the pertinent workspace. In other words under the conditions that the size of BP is held constant and  $\psi=0, \theta=0, \phi=0$ , changes in parameter  $(r_{end}/r_{base})$  has no effects on the volume of statically reachable combined workspace.

2) The statically reachable combined workspace volume with zero rotation of MP is dependent to the size of BP. In other words under the condition of  $\psi=0, \theta=0, \phi=0$ , changes in the parameter  $(r_{base}/r_{end})$  have positive effects on the statically reachable combined workspace, while increase in it leads to the increase of the workspace volume and as a result when the size of BP is increased, the workspace volume increases. This result is independent of ratio of MP/BP.

3) For maximum statically reachable combined workspace and under the condition of  $\psi=0, \theta=0, \phi=0$ , limit of  $(r_{base}/r_{end})=1$  does not exist.

4) It is proved that under the condition of holding  $r_{base}$  constant, the ratio of  $(r_{end}/r_{base})$  has no effects on the statically reachable combined workspace under the condition of  $\psi=0, \theta=0, \phi=0$ .

5) Change in parameter  $(r_{end}/r_{base})$  has no effect on the volume of wrench feasible workspace under the conditions of  $\psi=0, \theta=0, \phi=0$  and the applied moments on MP being zero. In other words under these conditions, change in the size of MP has no effect on the wrench workspace. By holding  $r_{end}$  constant, the reduction of forces  $f_x$  and  $f_y$  and increase in force  $f_z$ , increases the size of BP (increase of ratio  $(r_{base}/r_{end})$ ) and decrease in the angle  $\gamma$  results in the increase of workspace.

6) Change in parameter ( $r_{end}/r_{base}$ ) has effect on the volume of the wrench feasible workspace under conditions of constant applied force on MP, and variations of applied moments. The workspace of such robots in small magnitudes of moments  $M_x$  and  $M_y$ , is possible and in large magnitude of moment  $M_z$ . By holding  $r_{end}$  as constant, reduction of moments  $M_x$ ,  $M_y$  and  $M_z$  results in the increase of workspace and on the other hand changes in parameter ( $r_{base}/r_{end}$ ) have effect on the volume of wrench feasible workspace. Hence reduction of moments  $M_x$ ,  $M_y$  and  $M_z$  increases size of BP (increase of ratio of ( $r_{base}/r_{end}$ )) and size of MP (increase of ratio of ( $r_{end}/r_{base}$ )), and reduction of angle  $\gamma$  results in the increase of workspace.

REFERENCES

[1] Dagalakis, Nicholas G., Albus, James S., Wang, Ben-Li, Unger, Joseph, and Lee, James D., "Stiffness study of a parallel link robot crane for shipbuilding applications", *ASME Journal of Offshore Mechanics and Arctic Engineering*, 111(3), pp.183-193, August 1989.  
 [2] J.Hamedi, H.Zohoor, "Simulation and Optimization of the Rectangular Stewart Cable-Suspended Robot", *The 13th IASTED International Conference on Robotics, Applications and Telematics, Germany, Wurzburg, 2007*, pp. 400-407.  
 [3] Tanaka, M., Seguchi, Y., and Shimada, S., "Kineto-statics of skycam-type wire transport system", *In Proc. USA-Japan Symposium on Flexible Automation, Crossing Bridges:Minneapolis, Minnesota, 1988*, pp.689-694.  
 [4] Takeda, Y. and Funabashi, H., "Kinematic Synthesis of Spatial In-parallel Wire-Driven Mechanism with Six Degrees of Freedom with High Force Transmissibility", *Proceeding of ASME Design Engineering Technical Conferences, Baltimore, 2000*.  
 [5] Yang, L. F., Martin, M. M., and Chiou, J. C., "Stability and 3-D Spatial Dynamics Analysis of a Three Cable Crane", *American Society Aeronautics and Astronautics*, 2000, 2069-2076.  
 [6] Verhoeven, R., Hiller, M., and Tadokoro, S., "Workspace, Stiffness, Singularities and Classification of Tendon-Driven Stewart Platforms", *6th International Symposium on Robot Kinematics, Strobl, Austria, 1998*, pp.105-114.  
 [7] W. J. Shiang, D. Cannon, & J. Gorman, "Optimal force distribution applied to a robotic crane with flexible cables", *Proceeding of 2000 IEEE Conference on Robotics and Automation, San Francisco, California, 2000*, pp. 1948-1954.  
 [8] C.B. Pham, S.H. Yeo, G. Yang, M.Sh. Kurbanhusen, & I.M. Chen, "Force-Closure Workspace Analysis of Cable-Driven Parallel Mechanisms", *Mechanism and Machine Theory*, 41, pp.53-69, 2006.  
 [9] X. Diao, & O. Ma, "A method of verifying force-closure condition for general cable manipulators with seven cables", *Mechanism and Machine Theory*, 42, pp.1563-1576, 2007.

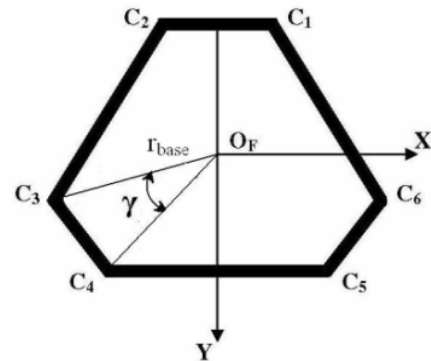


Fig. 2  $\gamma$  angle for BP

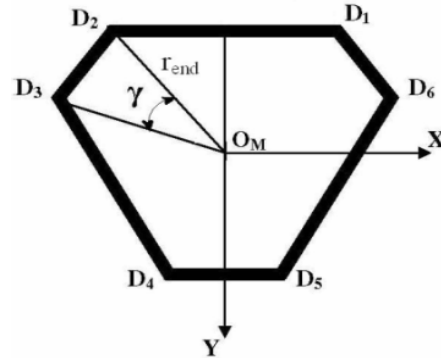


Fig. 3  $\gamma$  angle for MP

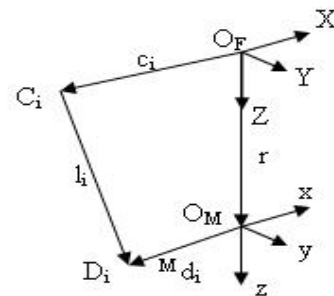


Fig. 4 vector polygon for  $i_{th}$  cable

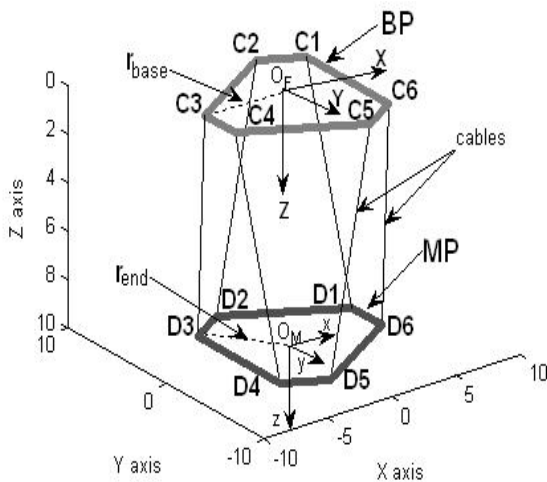


Fig.1 Used geometric model

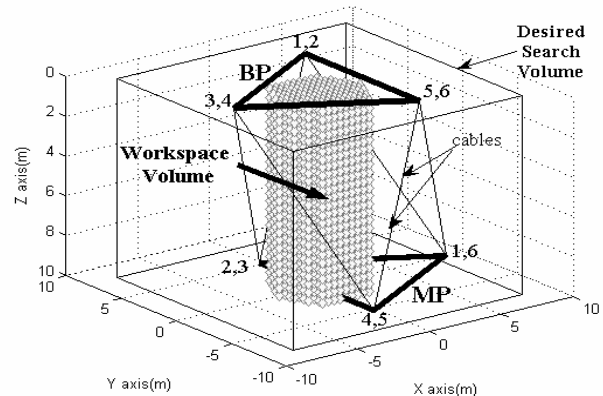


Fig. 5 statically reachable combined workspace for ( $r_{end}/r_{base}$ )=1 and configuration  $\gamma=0^\circ$

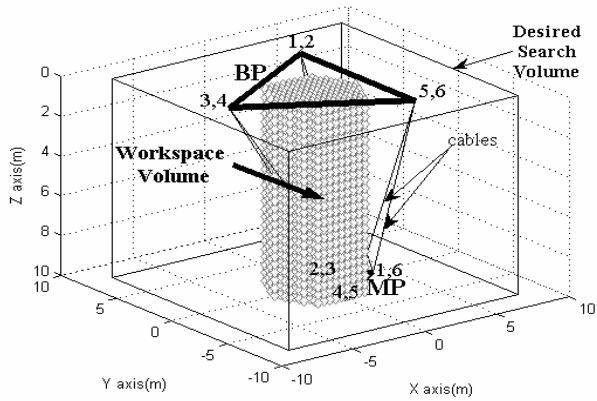


Fig. 6 statically reachable combined workspace for  $(r_{end}/r_{base})=0.2$  and configuration  $\gamma=0^\circ$

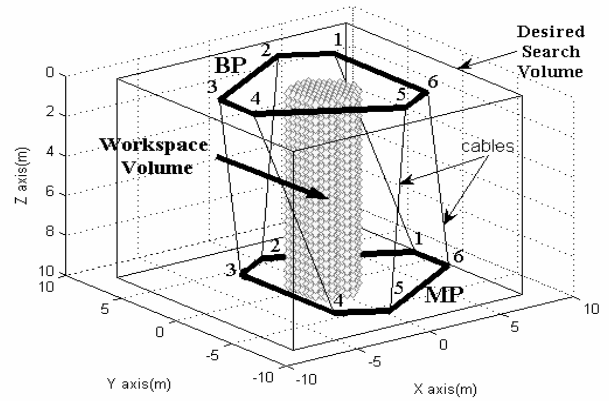


Fig. 9 statically reachable combined workspace for  $(r_{end}/r_{base})=1$  and configuration  $\gamma=30^\circ$

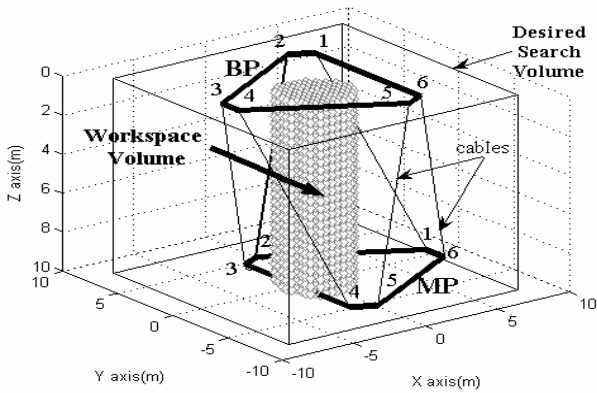


Fig. 7 statically reachable combined workspace for  $(r_{end}/r_{base})=1$  and configuration  $\gamma=15^\circ$

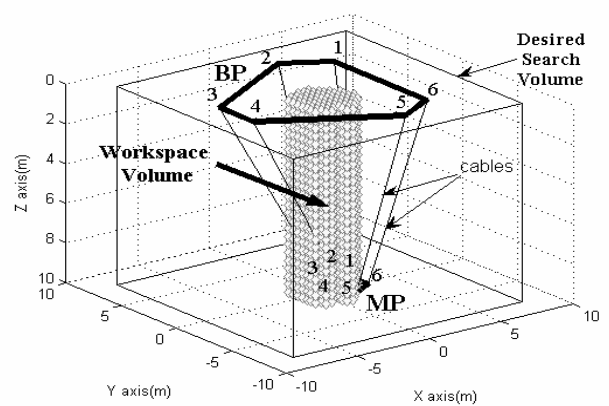


Fig. 10 statically reachable combined workspace for  $(r_{end}/r_{base})=0.2$  and configuration  $\gamma=30^\circ$

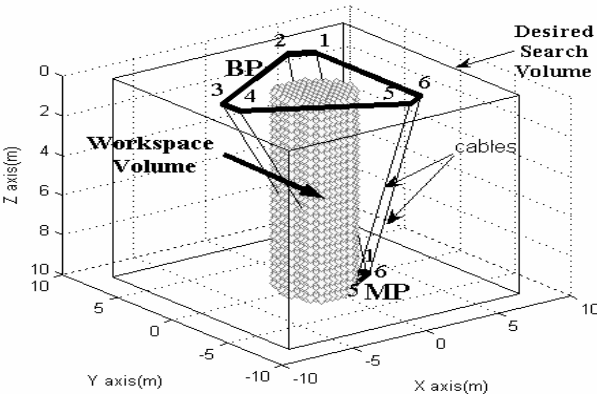


Fig. 8 statically reachable combined workspace for  $(r_{end}/r_{base})=0.2$  and configuration  $\gamma=15^\circ$

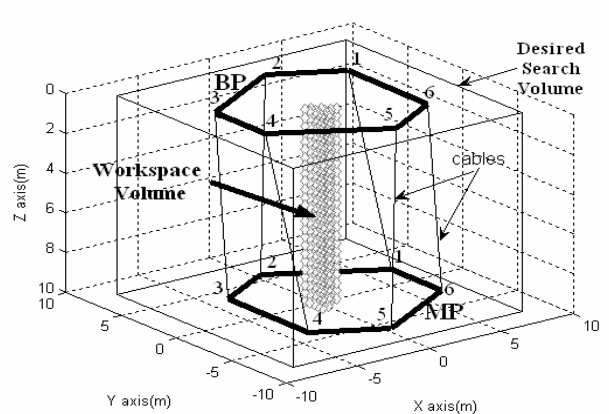


Fig. 11 statically reachable combined workspace for  $(r_{end}/r_{base})=1$  and configuration  $\gamma=45^\circ$

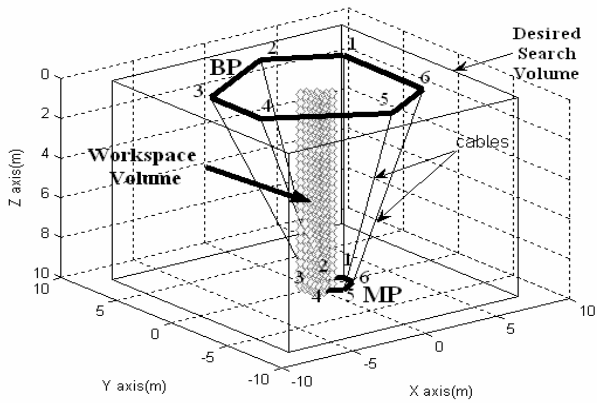


Fig. 12 statically reachable combined workspace for  $(r_{end}/r_{base})=0.2$  and configuration  $\gamma=45^\circ$

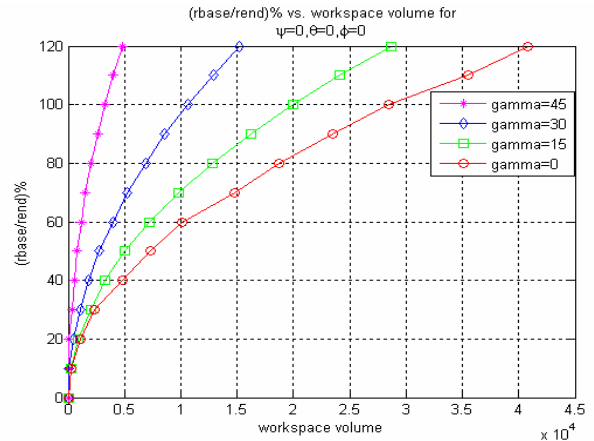


Fig. 15 The effect of the ratio of BP/MP on the basis of workspace volume

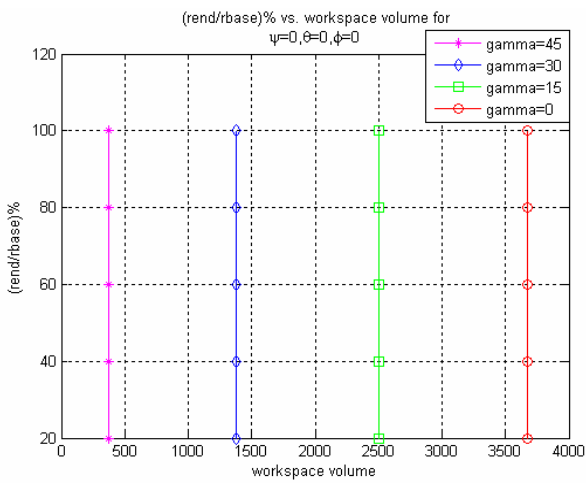


Fig. 13 The effect of the ratio of MP/BP on the basis of workspace volume

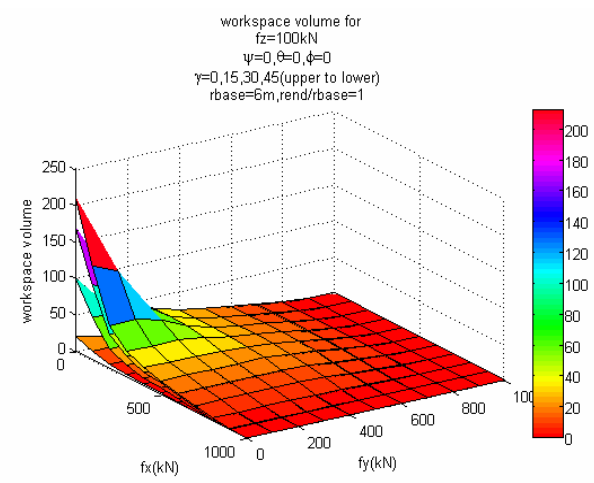


Fig. 16 Variation of  $f_x$  and  $f_y$  on the workspace volume for  $(r_{end}/r_{base})=1$

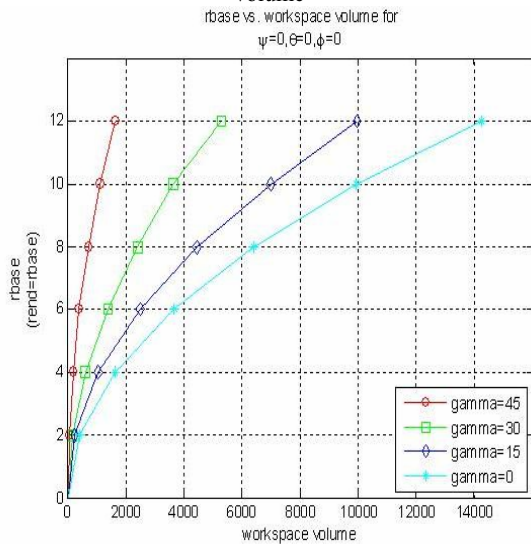


Fig. 14 The effect of the size of BP on the basis of workspace volume

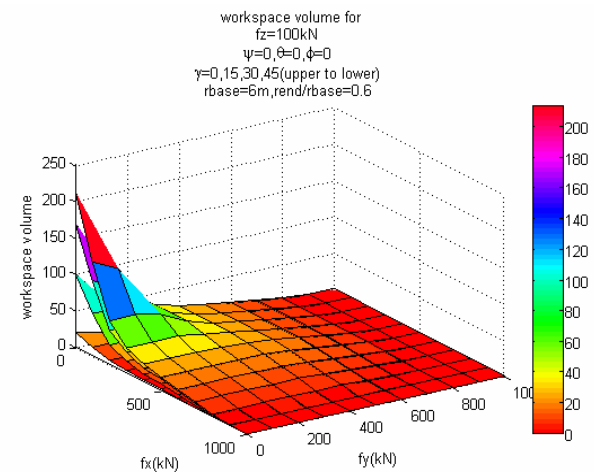


Fig. 17 Variation of  $f_x$  and  $f_y$  on the workspace volume for  $(r_{end}/r_{base})=0.8$



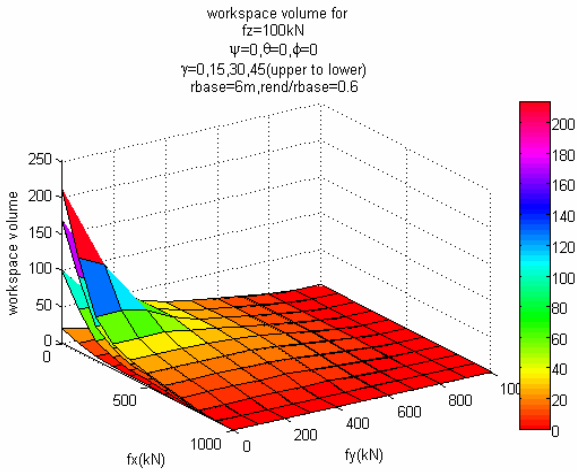


Fig. 18 Variation of  $f_x$  and  $f_y$  on the workspace volume for  $(r_{\text{end}}/r_{\text{base}})=0.6$

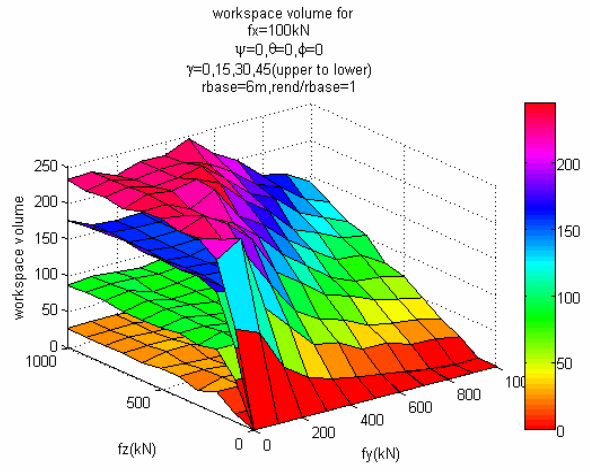


Fig. 21 Variation of  $f_y$  and  $f_z$  on the workspace volume for  $(r_{\text{end}}/r_{\text{base}})=1$

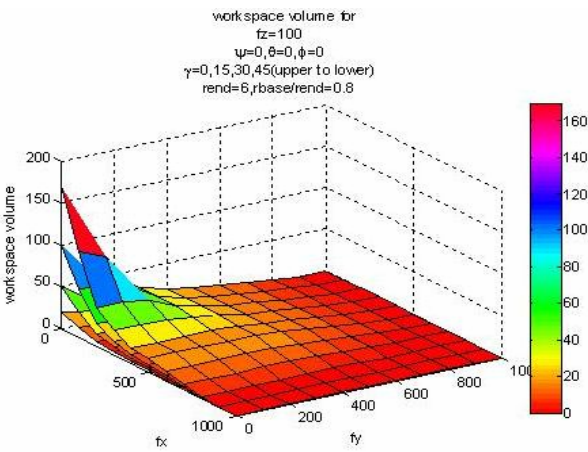


Fig. 19 Variation of  $f_x$  and  $f_y$  on the workspace volume for  $(r_{\text{base}}/r_{\text{end}})=0.8$

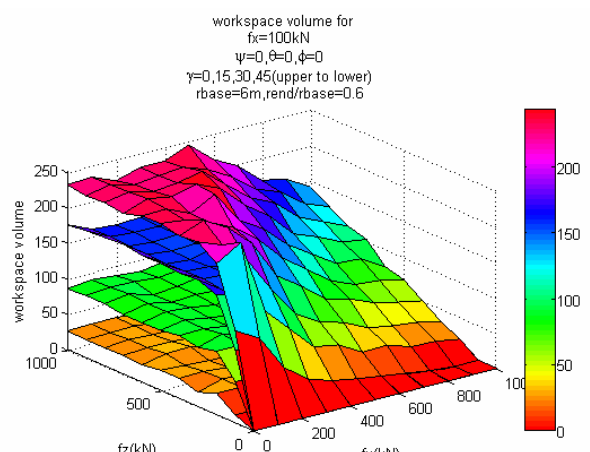


Fig. 22 Variation of  $f_y$  and  $f_z$  on the workspace volume for  $(r_{\text{end}}/r_{\text{base}})=0.6$

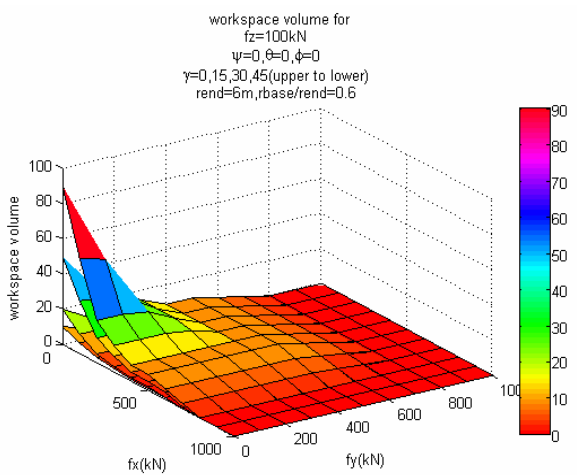


Fig. 20 Variation of  $f_x$  and  $f_y$  on the workspace volume for  $(r_{\text{base}}/r_{\text{end}})=0.6$

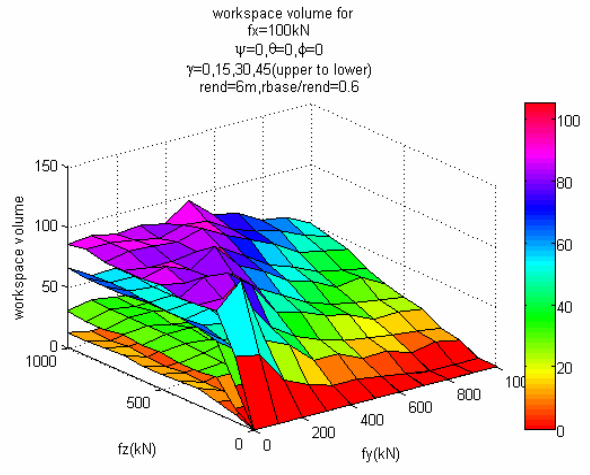


Fig. 23 Variation of  $f_y$  and  $f_z$  on the workspace volume for  $(r_{\text{base}}/r_{\text{end}})=0.6$

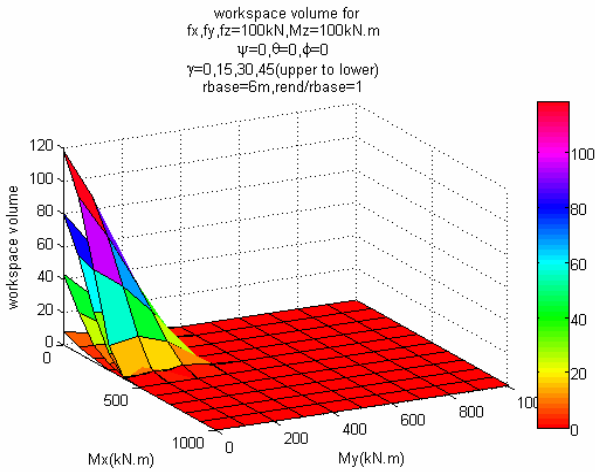


Fig. 24 Variation of  $M_x$  and  $M_y$  on the workspace volume for  $(r_{\text{end}}/r_{\text{base}})=1$

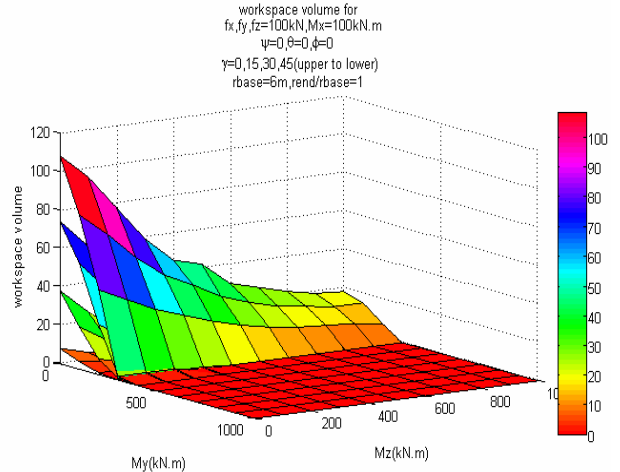


Fig. 27 Variation of  $M_y$  and  $M_z$  on the workspace volume for  $(r_{\text{end}}/r_{\text{base}})=1$

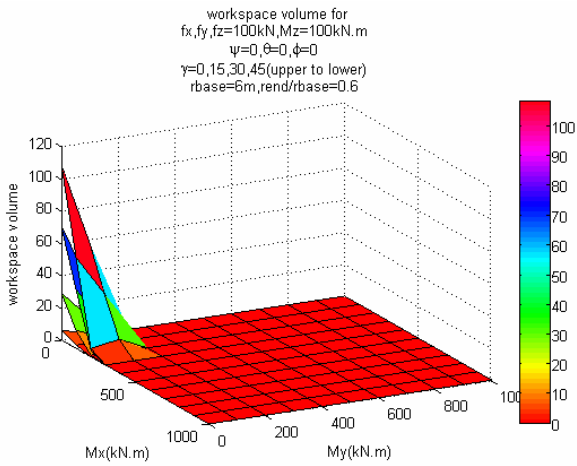


Fig. 25 Variation of  $M_x$  and  $M_y$  on the workspace volume for  $(r_{\text{end}}/r_{\text{base}})=0.6$

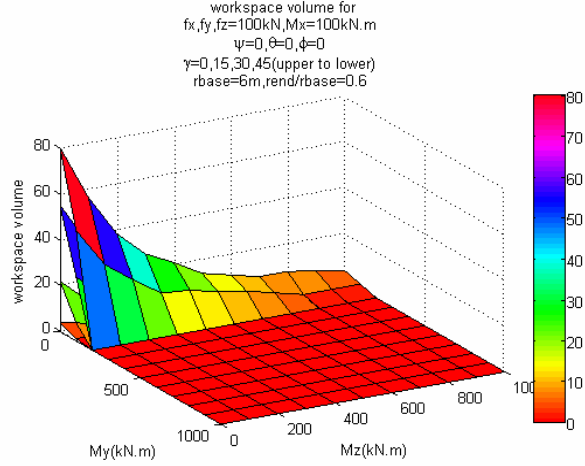


Fig. 28 Variation of  $M_y$  and  $M_z$  on the workspace volume for  $(r_{\text{end}}/r_{\text{base}})=0.6$

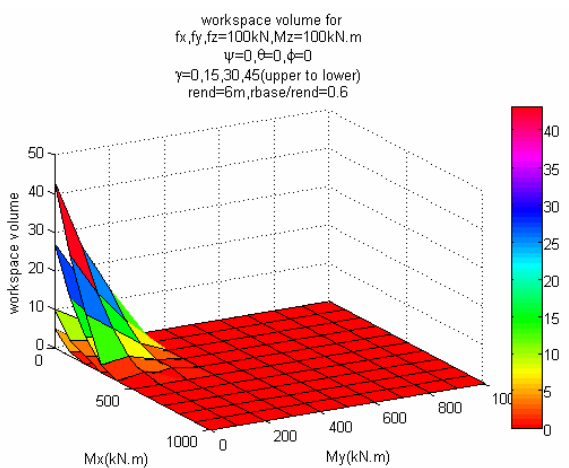


Fig. 26 Variation of  $M_x$  and  $M_y$  on the workspace volume for  $(r_{\text{base}}/r_{\text{end}})=0.6$

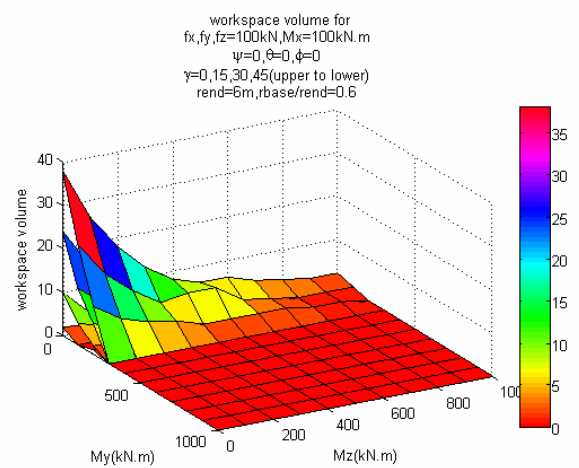


Fig. 29 Variation of  $M_y$  and  $M_z$  on the workspace volume for  $(r_{\text{base}}/r_{\text{end}})=0.6$